

Radiatively inefficient accretion flows induced by gravitational-wave emission before massive black hole coalescence

Kimitake Hayasaki

Department Astronomy, Kyoto University Oiwake-cho, Kitashirakawa, Sakyo-ku, Kyoto 606-8502

kimi@kusastro.kyoto-u.ac.jp

ABSTRACT

We study an accretion flow during the gravitational-wave driven evolution of binary massive black holes. After the binary orbit decays due to interacting with a massive circumbinary disk, the binary is decoupled from the circumbinary disk because the orbital-decay timescale due to emission of gravitational wave becomes shorter than the viscous timescale evaluated at the inner edge of circumbinary disk. During the subsequent evolution, the accretion disk, which is truncated at the tidal radius because of the tidal torque, also shrinks as the orbital decay. Assuming that the disk mass changed by this process is all accreted, the whole region of the disk completely becomes radiatively inefficient when the semi-major axis is several hundred Schwarzschild radii. The disk temperature can become comparable with the virial temperature there in spite of a low disk luminosity. The prompt high-energy emission is hence expected long before black hole coalescence as well as the gravitational wave signals. Binary massive black holes finally merge without accretion disks.

Subject headings: black hole physics - accretion, accretion disks - gravitational waves - galaxies: evolution - galaxies: active - galaxies: nuclei - quasars: general

1. Introduction

Astrophysical disks are ubiquitous and sources of active phenomena in the various system of the Universe; the star-compact object systems, star-planet systems, active galactic nuclei (AGNs), and so forth. Although the standard theory of accretion disks (Shakura & Sunyaev 1973) has succeeded in explaining them, there are still many unsolved problems.

High-energy emission from galactic black hole binaries and AGNs cannot be produced by the accretion flow derived from the standard disk theory, where radiative cooling is so

efficient that the thermal energy heated up by the viscosity is locally radiated away. If the radiative cooling becomes inefficient, the thermal energy is transported inward with accretion, and then the flow becomes hot. Such a flow can produce high-energy emission and is generally called as radiatively inefficient accretion flow (RIAF) (Chap. 9 of Kato et al. 2008).

The proto-type model of the RIAF is an optically thin advection-dominated accretion flow (ADAF)(Ichimaru 1977; Narayan&Yi 1994, 1995; Abramowicz et al. 1995; see also Chap. 9 of Kato et al. 2008 for a review). A low luminosity with high-energy emission can be explained by the ADAF with a significantly lower accretion rate than $\dot{M}_E = L_E/c^2 \sim 2 \times 10^{-2} M_7 [M_\odot \text{yr}^{-1}]$, where $L_E = 4\pi cGM_{\text{bh}}/\kappa_{\text{es}} \sim 1.3 \times 10^{45} M_7 [\text{ergs}^{-1}]$, c , G , M_7 , and κ_{es} are the Eddington luminosity, light speed, gravitational constant, black hole mass normalized by $10^7 M_\odot$, and electron scattering opacity, respectively. Observed power-law spectra of X-rays from Sgr A^* was well reproduced by ADAFs(Manmoto et al. 1997).

Most galaxies are thought to have massive black holes at their centers (Kormendy & Richstone 1995) and to coevolve with them(Magorrian et al. 1998; Ferrarese&Merritt 2000; Gebhardt et al. 2000). Galaxy merger leads to the mass inflow to the central region and then a nucleus of the merged galaxy is activated and black hole grows by gas accretion (Yu & Tremaine 2002).

During a sequence of processes, binary massive black holes with a sub-parsec scale separation are inevitably formed before two black holes merge by emitting gravitational radiation(Begelman et al. 1980; Escala et al. 2005; Dotti et al. 2007; Mayer et al. 2007). By interaction with surrounding stars (Merritt & Milosavljević 2005 and references therein; Sesana et al. 2007; Matsubayashi et al. 2007; Berentzen et al. 2009), gaseous disks(Ivanov et al. 1999; Gould & Rix 2000; Armitage & Natarajan 2002; Hayasaki 2009; Cuadra et al. 2009; Haiman et al. 2009), other massive black holes(Iwasawa et al. 2006), and infalling dwarf galaxies(Matsui & Habe 2009), the binary evolves towards coalescence within Hubble time in spite of being still extensive discussions(e.g., Lodato et al. 2009). Then, gravitational radiation emitted before the coalescence is detectable with the *Laser Interferometer Space Antenna*(LISA) and Pulsar Timing Arrays(PTAs).

An electromagnetic counterpart of gravitational wave signal plays a key role in localizing the source and determining its redshift. Some types of electromagnetic signatures has been studied such as afterglows(Milosavljević&Phinney 2005; Rossi et al. 2010; Corrales et al. 2010; Tanaka&Menou 2010) and precursors as the prompt emissions(Chang et al. 2009; Bode et al. 2010; Stone & Loeb 2010) and periodic emissions(Hayasaki et al. 2007, 2008; Bogdanović et al. 2008; MacFadyen & Milosavljević 2008; Hayasaki & Okazaki 2009).

In this Letter, we investigate RIAFs triggered by the rapid orbital decay due to emis-

sion of gravitational wave. The letter is organized as follows. The evolution of binary massive black holes interacting with a massive circumbinary disk are briefly described in Section 2. In Section 3, we derive the possible accretion flows and their luminosities during the gravitational-wave driven evolution. Section 4 is devoted to summary and discussion.

2. Final Parsec Evolution of Binary Massive Black Holes

We first briefly describe the evolution of binary massive black holes interacting with a massive circumbinary disk in the framework of coevolution of massive black holes and their host galaxies. The detailed description can be seen in Hayasaki et al. (2010).

Binary massive black holes are considered mainly to evolve via three stages (Begelman et al. 1980). Firstly, each of black holes sinks independently towards the center of the common gravitational potential due to the dynamical friction with neighboring stars. When the separation between two black holes becomes less than 1 pc or so, angular momentum loss by the dynamical friction slows down due to the loss-cone effect and a massive hard binary is formed. This is the second stage. The binary harden at the radius where the kinetic energy per unit mass of the star with the velocity dispersion equals to the binding energy per unit mass of the binary black hole(Quinlan 1996). Its hardening radius is defined as $a_h \sim 8.5 \times 10^{-1}[\text{pc}](q/(1+q)^2)M_7^{1-2/\beta_2}$, where $q = M_s/M_p$ is the ratio of primary black-hole mass, M_p , to secondary black-hole mass, M_s . Here, it is assumed that the total black-hole mass is tightly correlated with the velocity dispersion: $M_7 = \beta_1 (\sigma_*/200\text{kms}^{-1})^{\beta_2}$ with $\beta_1 = 16.6$ and $\beta_2 = 4.86$, where σ_* shows the one-dimensional velocity dispersion of stars(Merritt & Milosavljević 2005). Finally, the semi-major axis of the binary decreases to the radius at which the gravitational radiation dominates, and then a pair of black holes merge into a single, more massive one.

2.1. Triple-Disk Evolution

The circumbinary disk would be formed with hardening of the binary. The inner edge of circumbinary disk, r_{in} , is then defined as $r_{\text{in}} \approx 2a \sim 1.8[\text{pc}](q/(1+q)^2)M_7^{1-2/\beta_2}(a/a_h)$, where a is the semi-major axis of binary. For simplicity, the circumbinary disk is assumed to be a steady, axisymmetric, geometrically thin, self-regulated, self-gravitating but non-fragmenting with a Keplerian rotation and accretion rate, $\dot{M}_{\text{acc}} = (\eta/\epsilon)\dot{M}_{\text{Edd}}$, with the Eddington ratio, η and mass-to-energy conversion efficiency, ϵ .

The circumbinary disk and binary exchanges the energy and angular momentum through

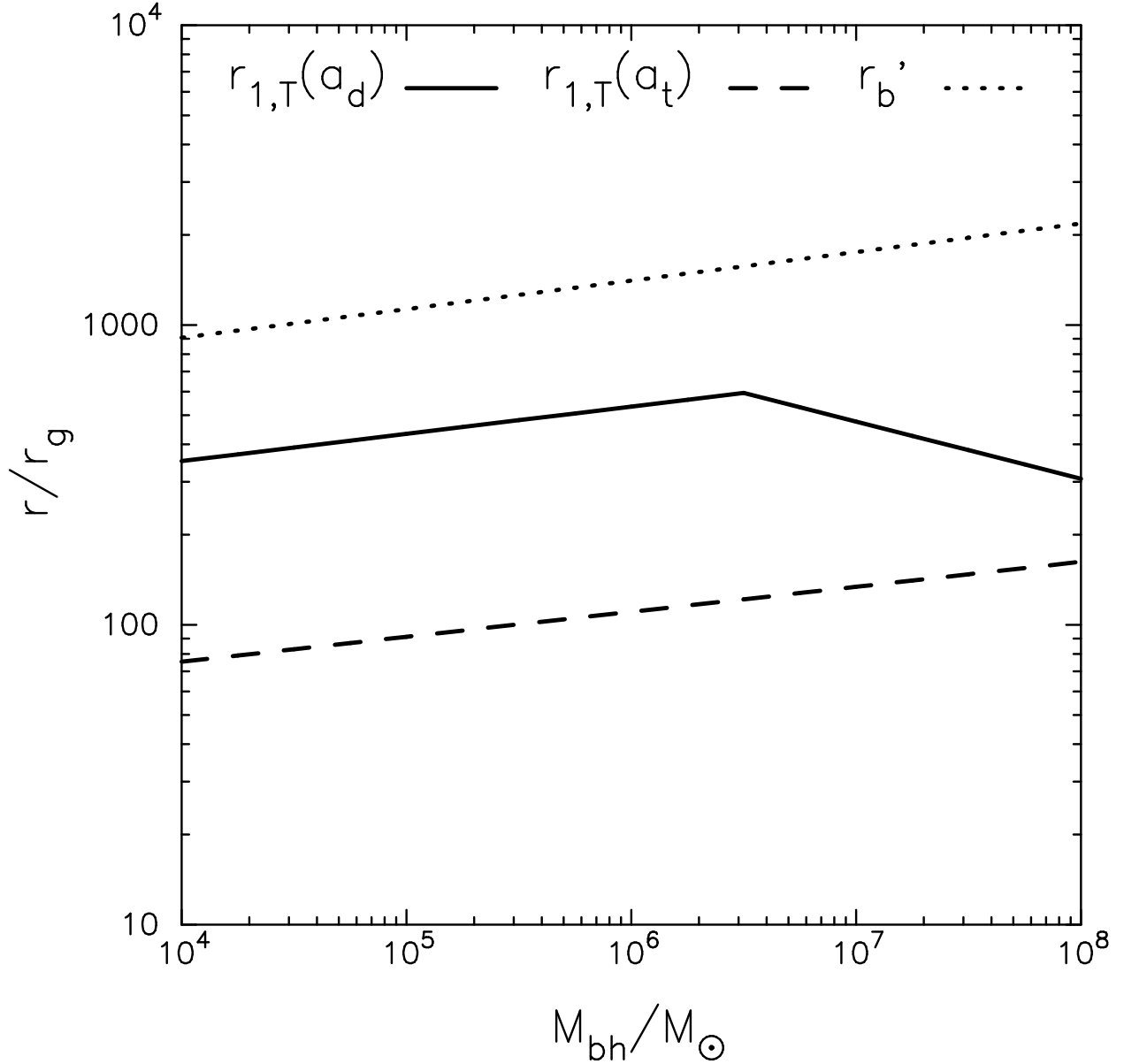


Fig. 1.— Black-hole mass dependence of characteristic radii of the accretion disk around the primary black hole in the case of the equal-mass binary. The solid line, dashed line, and dotted line show the tidal radius when the binary is decoupled from the circumbinary disk, transition radius from the standard disk to the RIAF when the transition radius corresponds to the tidal radius, and boundary between the inner region and the middle region in the standard disk at that time, respectively (see also equations (5), (12), and (11)).

the tidal/resonant interaction, which leads to the orbital decay of the binary. On the

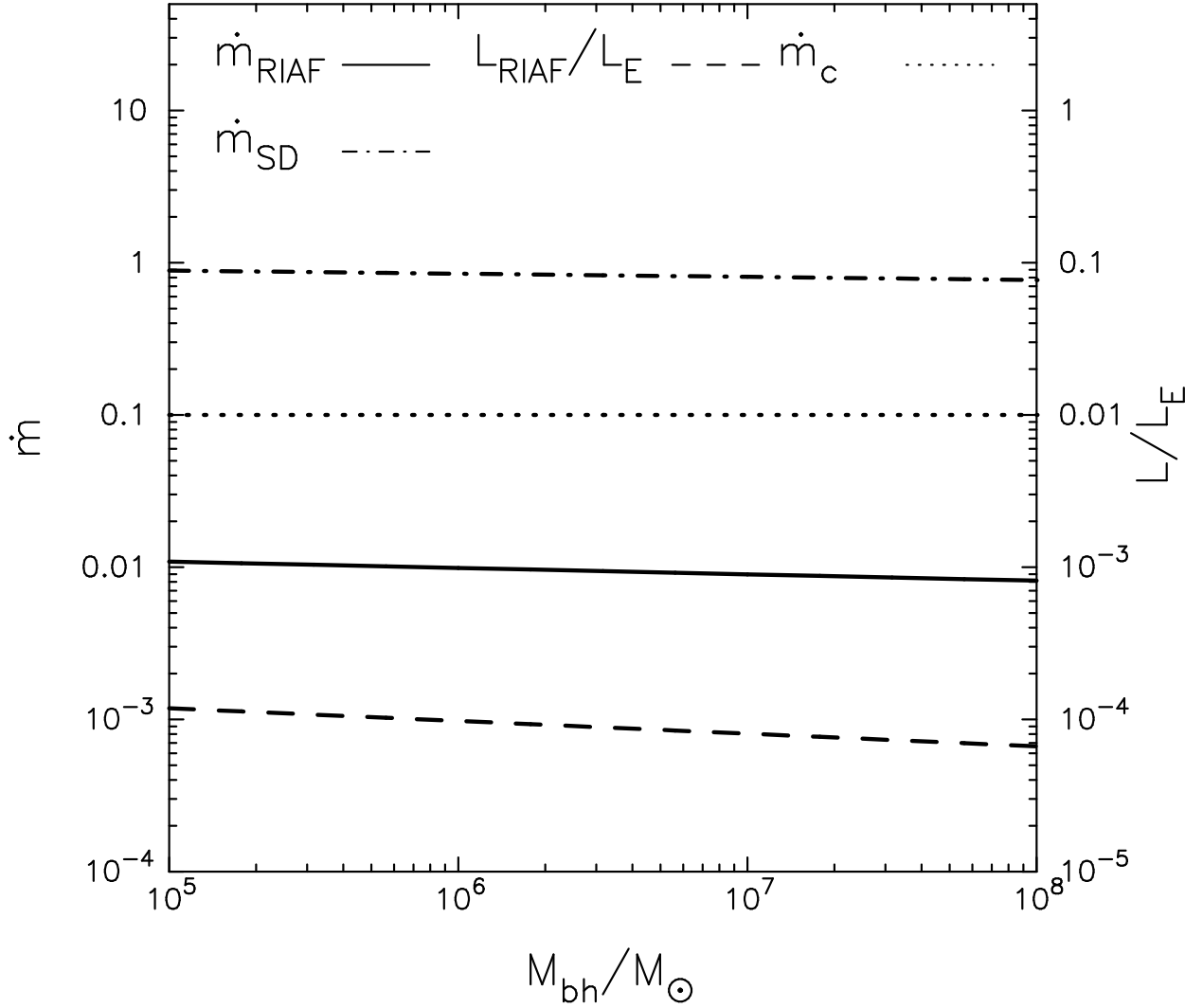


Fig. 2.— Black-hole mass dependence of the normalized accretion rate and corresponding normalized luminosity in the case of equal-mass binary. The solid line and dashed line show the normalized accretion rate, \dot{m}_{RIAF} , at the transition radius and corresponding normalized luminosity, L_{RIAF}/L_E , respectively. The dotted line shows the normalized critical accretion rate, \dot{m}_c . The dash-dotted line shows both the normalized accretion rate of standard, radiation-pressure dominated disk, \dot{m}_{SD} , at the transition radius and the corresponding normalized luminosity.

other hand, the gas at the inner edge of circumbinary disk overflows onto the central binary (Hayasaki et al. 2007). Then, an accretion disk is formed around each black hole (Hayasaki et al. 2008). The mass transfer therefore adds its angular momentum to the binary via accretion disks (Hayasaki 2009). In a steady state, the mass transfer rate equals to the accretion rate,

\dot{M}_{acc} . Since it is much smaller than the critical transfer rate defined by equation (41) of Hayasaki (2009), the effect of torque by the mass transfer torque can be neglected. Recently, Hayasaki et al. (2010) studied these processes in the framework of evolution of the binary to interact with the massive, non-isothermal circumbinary disk. The orbital-decay timescale is then given as

$$t_{\text{gas}} \sim 3.1 \times 10^8 [\text{yr}] \frac{q}{(1+q)^2} \eta_{0.1}^{-1} \epsilon_{0.1}, \quad (1)$$

where $\eta_{0.1} = \eta/0.1$ and $\epsilon_{0.1} = \epsilon/0.1$. The total mass-supply rate to the central binary is obtained as

$$M_{\text{sup}} = \dot{M}_{\text{acc}} t_{\text{gas}} \sim 6.2 \times 10^6 [M_{\odot}] M_7 \frac{q}{(1+q)^2}. \quad (2)$$

During the binary evolution, the total mass of two accretion disks must thus be less than M_{sup} . A mass of accretion disk around the primary black hole at the decoupling is defined by $M_{\text{ad}} = \int_{r_{\text{isco}}}^{r_{1,\text{T}}^{(\text{ad})}} \Sigma(r) r dr$ with equations (5) and (9) as an increasing function of black hole mass. Since $M_{\text{ad}} \lesssim 10^{-3} M_{\text{bh}}$ for $M_{\text{bh}} = 10^8 M_{\odot}$ and $q = 1$, M_{ad} is always less than M_{sup} over the whole mass range. Here, $r_{\text{isco}} = 3r_{\text{g}}$ with the Schwarzschild radius, $r_{\text{g}} = 2GM_{\text{bh}}/c^2$, shows the radius of innermost stable circular orbit around the Schwarzschild black hole.

2.1.1. Decoupling of Circumbinary Disk

The orbital-decay timescale of the binary by gravitational-wave emission can be written by Peters (1964) as

$$t_{\text{gw}} = \left| \frac{a}{\dot{a}} \right|_{\text{gw}} = \frac{5}{32} \left(\frac{a}{r_{\text{g}}} \right)^4 \frac{r_{\text{g}}}{c} \frac{(1+q)^2}{q} \frac{1}{f(e)}, \quad (3)$$

where $f(e) = (1 + 73e^2/24 + 37e^4/96)/(1 - e^2)^{7/2}$.

When the orbital-decay timescale is shorter than the viscous timescale measured at the inner edge of the circumbinary disk, the binary is decoupled from the circumbinary disk. The decoupling radius is then defined by Hayasaki et al. (2010) as

$$\frac{a_{\text{d}}}{r_{\text{g}}} = \begin{cases} [(32/5)(ct_{\text{vis,g}}/r_{\text{g}})(q/(1+q)^2)f(e)]^{4/11} \\ \text{for the standard disk} \\ [(32/5)(ct_{\text{vis,g}}/r_{\text{g}})(q/(1+q)^2)f(e)]^{2/7} \\ \text{for the self-gravitating disk} \end{cases}, \quad (4)$$

where $t_{\text{vis,g}}$ is the viscous timescale measured at $a = r_{\text{g}}$. For the standard disk, $t_{\text{vis,g}} \sim 5.9 \times 10^2 [\text{yr}] \alpha_{0.1}^{-1} \eta_{0.1}^{-1/4} \epsilon_{0.1}^{1/4} M_7^{5/4}$, where $\alpha_{0.1} = \alpha_{\text{SS}}/0.1$. For the self-gravitating disk, $t_{\text{vis,g}} \sim$

$5.6 \times 10^4 [\text{yr}] \alpha_{0.06}^{-1/3} \eta_{0.1}^{2/3} \epsilon_{0.1}^{2/3} M_7^{1/3}$, where $\alpha_{0.06} = \alpha_{\text{sg}}/0.06$. After the binary is decoupled from the circumbinary disk, the system consists of only an accretion disk around each black hole, and the orbital eccentricity gets rapidly close to zero with time.

3. Subsequent Double-Disk Evolution

For simplicity, we focus on the accretion disk around the primary black hole in what follows. Assuming that the binary has a circular orbit, the disk outer edge can be defined by the tidal radius as

$$r_{1,T}(a) \simeq 0.9R_1 \sim 0.42 \left(\frac{M_p}{M_p + M_s} \right)^{1/3} a, \quad (5)$$

where R_1 shows the inner Roche radius, which is approximately written as $R_1 = 0.462a/(q+1)^{1/3}$ for $q \gtrsim 0.1$ (e.g., Frank et al. 2002).

The logarithmic differentiation of equation (5) is given by

$$\frac{\dot{r}_{1,T}}{r_{1,T}} = \frac{\dot{a}}{a} + \frac{1}{3} \frac{q}{1+q} \left[\frac{\dot{M}_p}{M_p} - \frac{\dot{M}_s}{M_s} \right] \approx \frac{\dot{a}}{a}, \quad (6)$$

where \dot{M}_p and \dot{M}_s are the growth rate of primary black hole and that of secondary black hole, respectively. $\dot{M}_p/M_p \ll 1$ and $\dot{M}_s/M_s \ll 1$ are held during the evolution.

The accretion disk, which is truncated at the tidal radius because of its tidal torque, shrinks with the orbital decay due to gravitational-wave emission. The disk mass lying between $r + \Delta r$ and Δr can be then estimated as

$$\Delta M = 2\pi \int_r^{r+\Delta r} \Sigma(r) r dr \approx 2\pi r \Sigma(r) \Delta r. \quad (7)$$

We assume that the disk mass changed by shrinking of the tidal radius steadily accretes onto the black hole without being emitted as jet or wind. Combining equation (6) with equations (7) and (3), we then obtain the mass-accretion rate normalized by \dot{M}_E :

$$\dot{m} = \frac{2\pi r^2 \Sigma \dot{r}}{\dot{M}_E r} = \frac{2\pi r^2 \Sigma(r)}{t_{\text{gw}}} \frac{1}{\dot{M}_E} \quad (8)$$

Following Shakura & Sunyaev (1973), the standard disk structure has three different regions for a given mass accretion rate. At the present case, the outer region is neglected

because the disk outer edge is always less than the outer region. The surface density in the inner region and the middle region is written by Kato et al. (2008) as

$$\Sigma(r) = \begin{cases} \Sigma_{\text{in}}(r/r_g)^{3/2}\dot{m}^{-1}[\text{g/cm}^2] & r \leq r_b \\ \Sigma_{\text{mid}}(r/r_g)^{-3/5}\dot{m}^{3/5}[\text{g/cm}^2] & r \geq r_b \end{cases}, \quad (9)$$

where $\Sigma_{\text{in}} = 1.0 \times 10^2 \alpha_{\text{SS}}^{-1} f^{-1}$, $\Sigma_{\text{mid}} = 4.3 \times 10^{27/5} \alpha_{\text{SS}}^{-4/5} M_7^{1/5} f^{3/5}$ with $f = 1 - \sqrt{3r_g/r}$, and $r_b/r_g = 1.8 \times 10^{5/3} (\alpha_{\text{SS}} M_7)^{2/21} \dot{m}^{16/21}$ is the boundary between the inner region and the middle region.

From equations (8) and (9), we finally obtain the normalized accretion rate as

$$\dot{m} = \begin{cases} \left[(2\pi r_g^2 \Sigma_{\text{in}} / t_{\text{gw}}) \dot{M}_{\text{E}} \right]^{1/2} (r/r_g)^{7/4} & r \leq r'_b \\ \left[(2\pi r_g^2 \Sigma_{\text{mid}} / t_{\text{gw}}) / \dot{M}_{\text{E}} \right]^{5/2} (r/r_g)^{7/2} & r \geq r'_b \end{cases}, \quad (10)$$

where r'_b is a newly defined boundary between the inner region and middle region, which can be written as

$$\frac{r'_b}{r_g} = [(2\pi r_g^2)^{-8/7} \Sigma_{\text{in}}^{2/7} \Sigma_{\text{mid}}^{-10/7} / t_{\text{gw}}^{-8/7}] / \dot{M}_{\text{E}}^{-7/8}. \quad (11)$$

Next, we consider that the disk becomes a bimodal system of standard disk-RIAF, where the standard disk in the cool outer region transits to the RIAF in the inner hot region. We employ the transition radius, r_t , from the standard disk to the RIAF, defined by Homma (1996) as

$$\frac{r_t}{r_g} \approx 1.1 \times 10^{-2} \alpha_{0.1}^4 \epsilon_{0.1}^{-2} \dot{m}^{-2}. \quad (12)$$

Fig. 1 shows the mass dependence of characteristic radii of the accretion disk with $q = 1$. All the radii are normalized by the Schwarzschild radius. The solid line, dashed line, and dotted line show the tidal radius when the binary is decoupled from the circumbinary disk, transition radius when it corresponds to the tidal radius, and boundary between the inner region and the middle region of the accretion disk at that time, respectively. It is noted from the figure that the whole region of disk is completely radiatively inefficient when the disk-outer edge is a hundred Schwarzschild radius or so, which is less than the tidal radius when the binary is decoupled from the circumbinary disk. If the disk would still remain to be the standard disk at the transition radius, it is radiation-pressure dominated in the whole region of disk.

The corresponding luminosity of the RIAF normalized by the Eddington value can be written as(cf. Chap. 9 of Kato et al. 2008)

$$\frac{L}{L_E} \approx \epsilon \left(\frac{\dot{m}}{\dot{m}_c} \right) \dot{m}, \quad (13)$$

where $\dot{m}_c \sim \epsilon^{-1} \alpha^2$ is the critical accretion rate normalized by \dot{M}_E . There is no possible solution of RIAFs for $\dot{m} > \dot{m}_c$ (Narayan&Yi 1995). In contrast, the disk luminosity of the standard disk is written by $L/L_E = \epsilon \dot{m}$. Fig. 2 shows the mass dependence of the normalized accretion rate and corresponding normalized luminosity with $q = 1$. The solid line and dashed line show the normalized accretion rate at the transition radius and corresponding normalized luminosity, respectively. The normalized critical accretion rate is shown by the dotted line. The dash-dotted line shows both the normalized accretion rate of standard, radiation-pressure dominated disk at the transition radius and the corresponding normalized luminosity. It is noted from the figure that there is a possible solution for the RIAF because the normalized mass-accretion rate is about one order of magnitude lower than the normalized critical accretion rate. The normalized accretion rate of the RIAF and corresponding normalized luminosity are $\dot{m} \sim 10^{-2}$ and $L/L_E \sim 10^{-4}$, respectively, in the range from $10^5 M_\odot$ to $10^8 M_\odot$.

4. Summary&Discussion

We study radiatively inefficient accretion flows onto each black hole during the gravitational-wave emission driven evolution of binary massive black holes in the framework of coevolution of massive black holes and their host galaxies.

The binary system initially consists of the accretion disk around each black hole and the massive circumbinary disk surrounding them. After the binary is decoupled from the circumbinary disk, the outer edge of each accretion disk shrinks with the orbital decay due to emission of gravitational wave. Assuming that the disk mass changed by the rapid orbital decay is all accreted, the accretion flow is completely radiatively inefficient when the disk-outer edge corresponds to the transition radius from the standard disk to the RIAF. The normalized accretion rate of the RIAF and corresponding normalized luminosity are $\dot{m} \sim 10^{-2}$ and $L/L_E \sim 10^{-4}$, respectively. These values have little dependence on the black hole mass.

The virial temperature evaluated at the transition radius, $T_{\text{vir}} \sim GM_{\text{bh}} m_p / r_t$, is the order of 10^{10}K in the range from $10^5 M_\odot$ to $10^8 M_\odot$. The high-energy emission can therefore be expected in spite of a low luminosity and become a precursor of gravitational wave emitted

at black hole coalescence. Such a precursor leads to the merger of binary black holes with no accretion disks because all of disk materials are rapidly accreted at the precursor.

After two massive black holes merge into a single, more massive one due to the rapid orbital decay by gravitational-wave emission, gas in the decoupled circumbinary disk accretes onto the merged black hole. This produces the afterglow of the gravitational wave emitted at black hole coalescence (Milosavljević & Phinney 2005; Tanaka & Menou 2010). For $10^5 M_\odot$ black hole, the precursor occurs at $\sim 1.1 \times 10^2$ yr, when the orbital period of binary $\sim 1.3 \times 10^{-3}$ yr, and the subsequent afterglow occurs at $\sim 5.4 \times 10^2$ yr. The precursor could therefore give an evidence for such a very short orbital period binary.

K.H. is grateful to Loeb Abraham, Shin Mineshige, and Takahiro Tanaka for helpful discussions. The calculations reported here were performed using the facility at the Centre for Astrophysics & Supercomputing at Swinburne University of Technology, Australia and at YITP in Kyoto University. This work has been supported by the Grants-in-Aid of the Ministry of Education, Science, Culture, and Sport and Technology (MEXT; 19740100, 18104003, 21540304, 22540243, 22340045).

REFERENCES

- Abramowicz, M. A., Chen, X., Kato, S., Lasota, J.-P., & Regev, O. 1995, *ApJ*, 438, L37
- Armitage, P. J., & Natarajan, P. 2002, *ApJ*, 567, L9
- Begelman, M. C., Blandford, R. D., & Rees, M. J. 1980, *Nature*, 287, 307
- Berentzen, I., Preto, M., Berczik, P., Merritt, D., & Spurzem, R. 2009, *ApJ*, 695, 455
- Bode, T., Haas, R., Bogdanović, T., Laguna, P., & Shomarker, D. 2010, *ApJ*, 715, 1117
- Bogdanović, T., Smith, B. D., Sigurdsson, S., & Eracleous, M. 2008, *ApJ*, 174, 455
- Bogdanović, T., Eracleous, M., & Sigurdsson, S. 2009, *ApJ*, 697, 288
- Chang, P., Strubble, L.E., Menou, K., & Quataret E. 2009, arXiv0906.0825
- Cuadra, J., Armitage, P.J., Alexander, R.D., & Begelman, M.C. 2009, *MNRAS*, 393, 1423
- Corrales, L. R., Haiman, Z., & MacFadyen, A. 2010, *MNRAS*, 404, 947
- Dotti, M., Colpi, M., Haardt, F., & Mayer, L. 2007, *MNRAS*, 379, 956

- Dotti, M., Montuori, C., Decarli, R., Volonteri, M., Colpi, M., & Haardt, F. 2009, MNRAS, 389, 73
- Escala, A., Larson, R.B., Coppi, P.S., & Mardones, D. 2005, ApJ, 630,152
- Ferrarese, L., & Merritt, D. 2000, ApJ, 539, L9
- Frank, J., King, A., & Raine, D. *Accretion Power in Astrophysics* 3rd ed., (Cambridge University Press 2002).
- Gould, A., & Rix, H. 2000, ApJ, 532, L29
- Gebhardt., K. et al. 2000, ApJ, 539, L13
- Haiman, Z., Kocsis, B., & Menou, K. 2009, ApJ, 700, 1952
- Hayasaki, K., Mineshige, S., & Ho, C.L. 2008, ApJ, 682, 1134
- Hayasaki, K., Mineshige, S., & Sudou, H. 2007, PASJ, 59, 427
- Hayasaki, K. 2009, PASJ, 61, 427
- Hayasaki, K., & Okazaki, A.T. 2009, ApJ, 691, L5
- Hayasaki, K., Ueda, Y., & Isobe, N. 2010, PASJ, in press(arXiv1001.3612v2)
- Honma, F. 1996, PASJ, 48, 77
- Ichimaru, S. 1977, ApJ, 214, 840
- Ivanov, P. B., Papaloizou, J. C. B., & Polnarev, A. G. 1999, MNRAS, 307, 79
- Iwasawa, M., Funato, Y., & Makino, J. 2006, ApJ, 651, 1059
- Kato, S., Fukue, J., & Mineshige, S. *Black-Hole Accretion Disks*, (Kyoto Univ. Press. 2008).
- Kormendy, J., & Richstone, D. 1995, ARA&A, 33, 581
- Lodato, G., Nayakshin, S., King, A.R., & Pringle, J.E. 2009, 398, 1392
- Loeb, A. 2010, PhRvD, 81, 047503
- MacFadyen, I.A., & Milosavljević, M., 2008, ApJ, 672,83
- Magorrian, J., et al. 1998, AJ, 115, 2285
- Manmoto, T., Mineshige, S., & Kusunose, M, 1997, ApJ, 489, 791

- Matsui, M., & Habe, A. 2009, PASJ, 61, 421
- Matsubayashi, T., Makino, J., & Ebisuzaki, T. 2007, ApJ, 656, 879
- Mayer, L., Kazantzidis, S., Madau, P., Colpi, M., Quinn, T., & Wadsley, J. 2007, Science, 316, 1874
- Merritt, D., & Milosavljević, M. 2005, Living Rev. Relativity, 8, 8
- Milosavljević, M., & Phinney, E. S. 2005, ApJ, 622, L93
- Narayan, R., & Yi, I. 1994, ApJ, 428, L13
- Narayan, R., & Yi, I. 1995, ApJ, 452, 710
- Peters, P. C. 1964, Physical Review, 136, 1224
- Quinlan, G. D. 1996, New Astron. 1, 35
- Rossi, E. M., Lodato, G., Armitage, P.J., Pringle, J.E., & King A. R. 2010, MNRAS, 401, 2021
- Shakura, N. I., & Sunyaev, R. A. 1973, A&A, 24, 337
- Sesana, A., Haardt, F., & Madau, P. 2007, ApJ, 660, 546
- Stone, N., & Loeb, A. 2010, arXiv:1004.4833
- Tanaka, T., & Menou, K. 2010, ApJ, 714, 404
- Yu, Q., & Tremaine, S. 2002, MNRAS, 335, 965